Influence of Metal Precursor Chemistry and Calcination on NiFe-Based Electrocatalysts for the Oxygen Evolution Reaction

Sadeem AlOtaibi

KAUST Academy's Energy Transition Specialization Program

SadeemAbdullahX@hotmail.com

Abstract

Efficient OER electrocatalysts are essential for alkaline water electrolysis, but catalyst performance can depend strongly on how the material is prepared. This study examined the effects of precursor, solvent, and calcination on NiFe-based OER electrocatalysts. Eight catalysts were prepared using nitrate or acetylacetonate precursors in water or ethanol, with and without calcination at 450 °C. The uncalcined nitrate-based catalysts showed the best performance, with the water-based catalyst (N-W) reaching an overpotential of 515 mV at 100 mA cm^{-2} and a Tafel slope of 126.3 mV dec^{-1}. N-W also showed the lowest charge-transfer resistance (1.72 Ω). Notably, calcination generally decreased OER performance, indicating that thermal treatment was not required to achieve the best activity under the tested conditions. These results highlight a simple water-based, uncalcined approach as a promising route for preparing NiFe OER electrocatalyst.

Contents

1. Introduction 3

2. Methodology 4

2.1. Materials 4

2.2. Synthesis of NiFe Catalysts 5

2.3. Calculation 5

2.4. Characterization 5

2.5. Electrochemical Tasting 6

2.5.1. Electrode Preparation 6

2.5.2. Performance Testing 6

3. Results and Discussion 6

3.1. X-Ray Diffraction 6

3.2. OER Activity and Kinetics 7

3.3. Electrochemical Behavior 9

3.4. Stability 10

4. Conclusion 11

5. Acknowledgments 11

6. References 12

1. Introduction

The increasing demand for clean energy has driven interest in green hydrogen as a potential low-carbon energy carrier. Among the available hydrogen production methods, water electrolysis is an important approach for producing green hydrogen, particularly when powered by renewable electricity [1]. Through electrochemical water splitting, water can be converted into hydrogen and oxygen without direct carbon emissions, making water electrolysis an important technology in the transition toward cleaner energy systems [2].

Electrochemical water splitting consists of two simultaneous half-reactions: the hydrogen evolution reaction (HER), which occurs at the cathode and produces hydrogen, and the oxygen evolution reaction (OER), which occurs at the anode and produces oxygen. Although hydrogen is the desired product of water electrolysis, OER is considered the bottleneck of the overall process due to its sluggish kinetics and relatively high overpotential [3]. The OER involves a complex four-electron oxidation process, making it more kinetically demanding than HER. Therefore, reducing the overpotential and improving the kinetics of OER are important for increasing the efficiency of electrochemical water splitting and green hydrogen production [4].

In alkaline media, the OER proceeds through a series of surface reactions involving the adsorption and transformation of hydroxide species on active metal sites. Initially, hydroxide ions are adsorbed on the catalyst surface to form metal–hydroxyl (M–OH) species, followed by deprotonation to form M–O and subsequent formation of M–OOH intermediates. The M–OOH species then undergoes further reaction with hydroxide, leading to the formation and release of molecular oxygen. These sequential proton/electron transfer steps and surface intermediates contribute to the kinetic complexity of OER and influence the overall catalytic activity [5,6].

Effective OER electrocatalysts are important for reducing the energy requirements of water electrolysis. An ideal catalyst should exhibit high catalytic activity and stability while being based on earth-abundant, cost-effective, and environmentally suitable materials [7]. First-row transition-metal oxides, particularly those based on nickel, iron, cobalt, and manganese, have been widely investigated as OER catalysts for alkaline water electrolysis due to their favorable activity and abundance compared with noble-metal-based alternatives.

Among first-row transition-metal-based OER catalysts, nickel–iron (NiFe) materials, particularly NiFe layered double hydroxides (NiFe LDHs) and iron-incorporated nickel compounds, have received significant attention for alkaline OER [8,9]. NiFe-based catalysts can be synthesized through various approaches, including co-precipitation [10], electrodeposition [11], and hydrothermal or solvothermal methods. Commonly reported metal

precursors include nitrate [12], sulfate, acetylacetonate, and chlorides, while different reaction media have been employed under a range of synthesis conditions.

The synthesis conditions of NiFe-based catalysts can influence their structural and physicochemical properties, which may subsequently affect their electrochemical performance [13,14]. In particular, the choice of metal precursor and reaction solvent can influence the formation and characteristics of the resulting NiFe material, while post-synthesis thermal treatment can alter its crystallinity and phase composition. Understanding these effects is therefore important when comparing NiFe catalysts prepared through different synthesis routes.

Precursor type, solvent, and thermal treatment provide three key variables for comparing NiFe catalyst preparation routes. Metal acetylacetonates are commonly used with organic solvents such as ethanol, whereas nitrate salts are readily soluble in water and can provide an alternative water-based synthesis route [15,16]. Comparing these precursor systems using the same solvent conditions provides an opportunity to examine whether precursor and solvent selection influence the resulting catalyst properties and OER performance. In addition, nitrate-based precursors have been reported in synthesis routes that do not require extensive thermal treatment, offering the potential for a simpler preparation process. Therefore, both calcined and uncalcined catalysts were considered to evaluate the effect of thermal treatment alongside precursor and solvent selection.

This project aims to systematically investigate how different nickel and iron precursors (acetylacetonate and nitrate salts), solvents (water and ethanol), and calcination versus non-calcination routes affect the physicochemical properties and electrochemical performance of NiFe-based catalysts for the oxygen evolution reaction.

2. Methodology

2.1. Materials

All chemicals were of analytical grade and used without further purification. Nickle (II) Acetylacetonate 95% ($Ni(C_5H_7O_2)_2$, mw: 256.91g/mol), and Iron (III) Acetylacetonate 98% ($Fe(C_5H_7O_2)_3$, mw: 353.17g/mol) were obtained from Aladdin Scientific. Nickel (II) Nitrate Hexahydrate 99.8% ($Ni(NO_3)_2{\cdot}6H_2O$, mw: 290.80g/mol) from Alfa Aeser. Both Iron (III) Nitrate Nonahydrate 99.9% ($Fe(NO_3)_2{\cdot}9H_2O$, mw: 404g/mol) and Urea 99% (mw: 60.06g/mol) were purchased from Macklin. Ethanol 96% and distilled water were used throughout the experiments.

2.2. Synthesis of NiFe Catalysts

NiFe catalysts were synthesized via a hydrothermal route using different precursor–solvent combinations with a fixed Ni:Fe molar ratio of 3:1. Four primary formulations were prepared: nickel and iron acetylacetonates in ethanol (Ac-Et) or water (Ac-W), and nickel and iron nitrates in ethanol (N-Et) or water (N-W). In a typical synthesis, the nickel precursor (130 mg) and iron precursor (60 mg) were dissolved in 70 mL of the respective solvent and stirred for 30 min at room temperature. Urea (80 mg) was added, and the mixture was stirred for an additional 2 h before being transferred into a 100 mL Teflon-lined stainless-steel autoclave and heated at 200°C for 12 h. After natural cooling, the precipitate was collected by centrifugation, washed three times with ethanol (10,000 rpm, 5 min/cycle), and dried at 80°C for 2 h. The resulting dried powder was stored for analysis.

To investigate the effect of calcination, a portion of each catalyst was calcined in a split-tube furnace at 450°C for 5 h at the rate of 10°C min^{-1}. The corresponding calcined catalysts were denoted as Ac-EtC, Ac-WC, N-EtC, and N-WC, yielding a total of eight sample variations.

2.3. Calculation

2.3.1 Potential Conversion to RHE

All measured potentials ($E_{Ag/AgCl}$) were converted to the Reversible Hydrogen Electrode (RHE) scale using the Nernst equation (1):

$$E_{RHE} = E_{Ag/AgCl} + E^{o}_{Ag/Agcl} + (0.0591 \times pH) \quad (1)$$

Where $E^{o}_{Ag/AgCl}$ = 0.197V for saturated KCl and pH = 13.6 for 1M KOH electrolyte.

2.3.2. *i*R-Compensation

To account for ohmic losses caused by the uncompensated electrolyte resistance R_s, an 85% *i*R-correction was applied using the following formula:

$$E_{RHE,85\%corr} = E_{RHE} - (\frac{I_{(mA)}}{1000} \times 0.85 \times R_s) \quad (2)$$

2.4. Characterization

X-Ray Diffraction (XRD) analysis was conducted using Bruker D2 Phaser, with Cu Kα radiation (1.54184Å) at 30kV, 10mA, with 0.01° step size and 2θ scan range from 5° to 90°.

2.5. Electrochemical Tasting

2.5.1. Electrode Preparation

The catalyst ink was prepared by dispersing 5 mg of catalyst powder in a microcentrifuge tube containing 1000 μL of ethanol and 30 μL of Nafion solution (5 wt%). The mixture was ultrasonicated for 30-45 min to obtain a homogeneous suspension. The resulting ink was uniformly spray-coated onto a 1 × 1 cm^2 carbon paper substrate mounted on a heated plate maintained at 40–55°C to promote rapid solvent evaporation and ensure a uniform active layer.

2.5.2. Performance Testing

All electrochemical measurements were carried out with an electrochemical workstation (BioLogic SP-150 Potentiostat) at room temperature. A standard three-electrode system was used for this study. The as prepared electrode was used as working electrode, a platinum foil and an Ag/AgCl (saturated KCl) electrodes were used as counter electrode and reference electrode, respectively. Cyclic Voltammetry (CV) was conducted for 30 continuous cycle to clean and activate the surface of the catalyst. Potentiostatic Electrochemical Impedance Spectroscopy (PEIS) was performed following CV activation across a frequency range of 200 kHz to 100 mHz to measure the solution resistance R_s. Linear Sweep Voltammetry (LSV) was subsequently recorded at a sweep rate of 10 mV/**s** across the OER potential region. Scans were recorded in triplicate to ensure reproducibility. A chronopotentiometry (CP) analysis with a fixed current density of 100 mA was applied to evaluate the stability of the catalyst for 100h.

3. Results and Discussion

3.1. X-Ray Diffraction

The XRD patterns of the synthesized NiFe-based catalysts are shown in **Figure 1**. The uncalcined samples exhibit relatively broad and weak diffraction features, including reflections at low diffraction angles. These low-angle features are consistent with the characteristic reflections reported for NiFe layered double hydroxide (LDH) structures, with reported NiFe LDH reflections occurring at approximately 11° and 22° [17,18]. Therefore, the presence of these features suggests the possible formation of NiFe hydroxide/LDH-like phases in the as-synthesized materials. Upon calcination, the diffraction peaks become sharper and more pronounced, indicating increased crystallinity and structural transformation during thermal treatment. The low-angle reflections observed in the uncalcined samples are no longer apparent after calcination, further supporting a structural transformation of the as-synthesized hydroxide/LDH-like phases. The observed reflections in the calcined samples show correspondence with the reference patterns of NiO, Fe_3O_4, and Fe_2O_3, suggesting the formation

of Ni- and Fe-containing oxide phases. Differences in peak intensity and appearance among the samples also indicate that precursor chemistry and solvent conditions influence the resulting crystalline structure.

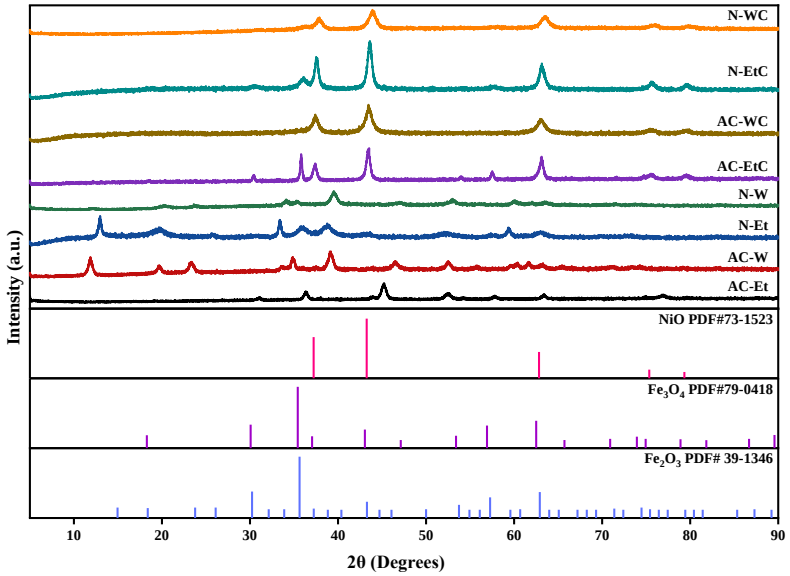


***Figure 1**. XRD patterns of the NiFe electrocatalysts before and after calcination at 450 °C, with calcined samples shown above and uncalcined samples below, alongside reference patterns (2θ = 5–90°).*

3.2. OER Activity and Kinetics

The OER activity of the synthesized electrocatalysts was first evaluated using linear sweep voltammetry (LSV), shown in **Figure 2**, with the corresponding overpotential values summarized in **Table 1**. At the benchmark current density of 100 mA/cm^2 the uncalcined nitrate-based samples, N-W (nitrate precursor in water) and N-Et (nitrate precursor in ethanol), demonstrated the superior electrocatalytic activity, requiring overpotentials of only 515 mV and 614 mV, respectively. These were followed by the calcined nitrate-in-water sample (N-WC), whereas acetylacetonate-derived catalysts exhibited substantially higher overpotentials across all tested conditions. Across the entire dataset, nitrate-based electrocatalysts consistently outperformed their acetylacetonate counterparts. At the higher current density of 500 mA/cm², N-W also showed the lowest η (670 mV), followed by N-Et (1054 mV), N-WC (1140 mV).

Furthermore, thermal treatment at 450 °C negatively impacted performance, as calcination caused a clear increase in overpotential and a reduction in catalytic activity across most catalyst formulations. A unique trend was observed for AC-WC, where calcination initially improved performance at lower current densities, reducing the η_{100} from 1069 mV (AC-W) down to 940 mV. However, calcination severely degraded the polarization slope of AC-WC at higher current densities indicating increased mass-transport resistance or limited charge-transfer kinetics at elevated reaction rates post-calcination.

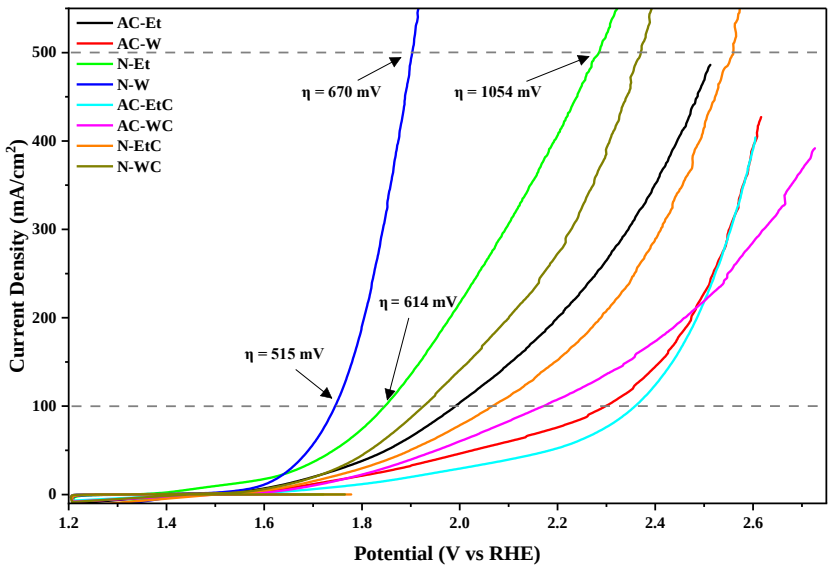


Figure 2. *Linear sweep voltammetry (LSV) polarization curves of as-synthesized and calcined NiFe electrocatalysts recorded in 1.0 M KOH at a scan rate of 10 mVs^{-1}.*

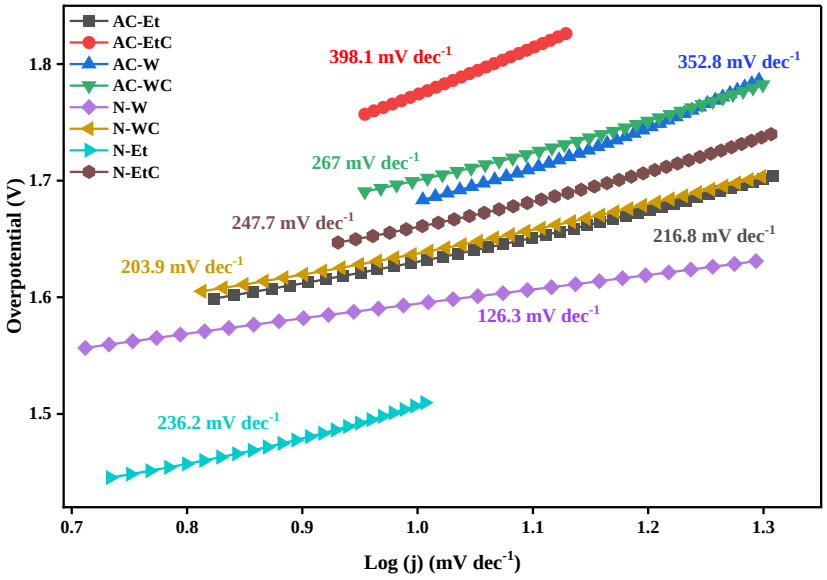


Figure 3*. Tafel plots of the NiFe electrocatalysts derived from LSV polarization curves in 1.0 M KOH.*

The Tafel slopes obtained from the linear regions of the polarization curves are shown in **Figure 3**, and summarized in **Table 1**. N-W exhibited the lowest Tafel slope of 126.3 mV dec^{-1}, indicating the most favorable OER kinetics among the investigated catalysts. The nitrate-based catalysts generally showed lower Tafel slopes than the corresponding acetylacetonate-based catalysts, particularly for the water-based samples. Calcination at 450 °C increased the Tafel slope for the nitrate-water catalyst from 126.3 to 203.9 mV dec^{-1}, indicating a decrease in kinetic performance after thermal treatment. A similar increase was observed for the ethanol-based nitrate catalyst, from 236.2 to 247.7 mV dec^{-1}. In contrast, calcination reduced the Tafel

slope of the acetylacetonate-based catalysts, from 352.8 to 267.0 mV dec^{-1} for the water-based samples and from 216.8 to 398.1 mV dec^{-1} for the ethanol-based samples.

Table 1. *Summary of OER electrochemical performance parameters for all NiFe-based catalyst variants in 1.0M KOH.*

Catalyst	Precursor	Solvent	Calcination (450 °C)	Overpotential at 100 mA/cm^2, η_{100} (mV)	Overpotential at 500 mA/cm^2, η_{500} (mV)	Tafel slop (mV dec^{-1})
N-W	Nitrate	Water	No	**515**	670	126.3
N-WC	Nitrate	Water	Yes	695	1140	203.9
N-Et	Nitrate	Ethanol	No	614	1054	236.2
N-EtC	Nitrate	Ethanol	Yes	834	1320	247.7
Ac-W	Acetylacetonate	Water	No	1069	-	352.8
Ac-WC	Acetylacetonate	Water	Yes	940	-	267
Ac-Et	Acetylacetonate	Ethanol	No	761	-	216.8
Ac-EtC	Acetylacetonate	Ethanol	Yes	1128	-	398.1

3.3. Electrochemical Behavior

Potentiostatic electrochemical impedance spectroscopy (PEIS) was performed to evaluate interfacial charge-transfer kinetics, as shown in **Figure 4**. Solution resistance (Rs), measured from the high-frequency X-intercept, remained low across all samples (0.7-2.0 Ω).

Charge-transfer resistance (R_{ct}), determined by the semicircle diameter along the real impedance axis (Z'), mirrored the LSV performance trends. Uncalcined nitrate catalysts exhibited the lowest charge-transfer barriers: N-W recorded the smallest R_{ct} at 1.72 Ω, followed by N-Et at 2.75 Ω. This minimal resistance accounts for their lower η_{100} of 515 mV and 614 mV, respectively, and fastest charge-transfer [19].

Calcination at 450 °C increased interfacial resistance across all samples. For instance, calcining N-W to N-WC tripled R_{ct} to 5.21 Ω, while N-EtC increased to 8.91 Ω. Among the acetylacetonate series, uncalcined variants showed moderate resistance (AC-Et at 7.28 Ω and AC-W at 14.2 Ω), whereas calcination (AC-EtC) resulted in a dramatic expansion of the Nyquist arc to 53.5 Ω, providing a direct physical basis for its sluggish OER kinetics.

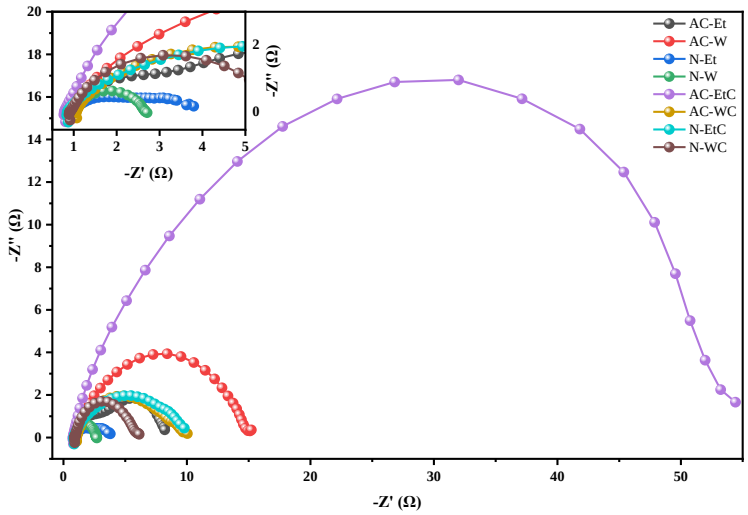


Figure 4. *Nyquist plots of the NiFe electrocatalysts obtained by electrochemical impedance spectroscopy (EIS) in 1.0 M KOH, with an enlarged view of the 0–5 Ω region shown in the inset.*

3.4. Stability

Chronopotentiometric stability tests of N-W and N-Et, **Figure 5**, showed relatively stable potentials during much of the measurement period, indicating sustained OER operation under the applied current density. N-W maintained a stable potential for approximately 50 h before a sharp increase was observed, whereas N-Et remained stable for over 75 h before a similar increase. The gradual stability followed by a rapid potential increase may indicate deterioration of the electrode during prolonged operation, although contributions from electrode detachment, bubble accumulation, or mass-transport limitations cannot be excluded. Despite N-W exhibiting superior initial OER activity in the LSV measurements, N-Et demonstrated longer stable operation under the tested conditions.

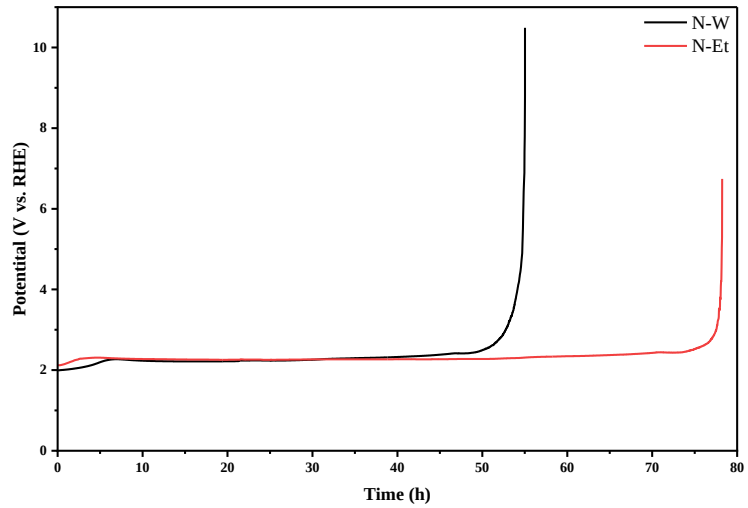


Figure 5. *Chronopotentiometry of N-W and N-Et catalysts at a constant current density of 100 mA cm⁻² for 100 h in 1.0 M KOH.*

4. Conclusion

This study investigated the influence of precursor type, solvent, and calcination on the structural and electrochemical properties of NiFe-based electrocatalysts for the oxygen evolution reaction (OER). Eight catalyst variants were synthesized using nickel and iron nitrate or acetylacetonate precursors in water or ethanol, with and without calcination at 450 °C. The results demonstrated that both precursor chemistry and thermal treatment significantly affected the resulting catalyst structure and OER performance.

XRD analysis indicated that the uncalcined materials exhibited features consistent with NiFe hydroxide/LDH-like structures, while calcination resulted in structural transformation toward Ni- and Fe-containing oxide phases. Electrochemical measurements showed that the nitrate-based catalysts generally exhibited superior OER performance compared with the acetylacetonate-based catalysts. Among all samples, the uncalcined nitrate-in-water catalyst (N-W) demonstrated the best overall activity, requiring an overpotential of 515 mV at 100 mA cm^{-2} and exhibiting the lowest Tafel slope of 126.3 mV dec^{-1}. EIS measurements supported these findings, with N-W showing the lowest charge-transfer resistance (1.72 Ω).

Calcination at 450 °C generally resulted in decreased OER performance, as reflected by increased overpotentials, higher Tafel slopes, and increased charge-transfer resistance for most catalyst formulations. This indicates that the thermal treatment and associated structural transformation were not beneficial for the electrochemical performance under the conditions investigated. The stability measurements further revealed a difference between initial activity and long-term operation: N-W showed superior initial OER activity but experienced a potential increase after approximately 50 h, whereas N-Et maintained relatively stable operation for more than 75 h. Overall, the findings demonstrate that precursor and solvent selection can play a significant role in determining the structural and electrochemical properties of NiFe OER electrocatalysts, with the uncalcined nitrate-based materials showing the most favorable performance among the investigated samples.

5. Acknowledgments

I would like to thank KAUST Academy and K.A.CARE for providing me with the opportunity to undertake this research experience. I am especially grateful to Dr. Abdul Malek for his guidance, support, and valuable feedback throughout this project, and to Prof. Xu Lu and the members of his research group for providing a supportive research environment and assistance throughout the work.

6. References

[1] H.A. Younus, R. Al Hajri, N. Ahmad, N. Al-Jammal, F. Verpoort, M. Al Abri, Green hydrogen production and deployment: opportunities and challenges, Discover Electrochemistry 2 (2025). https://doi.org/10.1007/s44373-025-00043-9.

[2] Y. Wang, Y. Zhou, X. Zhao, Y. Guo, Z. He, S. Ma, B. Xu, X. Hao, Boosting oxygen evolution activity via Cr-induced electronic and structural modulation in NiFe-LDH nanosheets, CrystEngComm (2026). https://doi.org/10.1039/d6ce00303f.

[3] G.A. Gebreslase, M.V. Martínez-Huerta, M.J. Lázaro, Recent progress on bimetallic NiCo and CoFe based electrocatalysts for alkaline oxygen evolution reaction: A review, Journal of Energy Chemistry 67 (2022) 101–137. https://doi.org/10.1016/j.jechem.2021.10.009.

[4] A. Zuber, I.M. Oikonomou, L. Gannon, I. Chunin, L. Reith, B. Can, M. Lounasvuori, T. Schultz, N. Koch, C. McGuinness, P.W. Menezes, V. Nicolosi, M.P. Browne, Effect of the Precursor Metal Salt on the Oxygen Evolution Reaction for NiFe Oxide Materials, ChemElectroChem 11 (2024). https://doi.org/10.1002/celc.202400151.

[5] N.T. Suen, S.F. Hung, Q. Quan, N. Zhang, Y.J. Xu, H.M. Chen, Electrocatalysis for the oxygen evolution reaction: Recent development and future perspectives, Chem. Soc. Rev. 46 (2017) 337–365. https://doi.org/10.1039/c6cs00328a.

[6] A. Malek, Y. Xue, X. Lu, Dynamically Restructuring NixCryO Electrocatalyst for Stable Oxygen Evolution Reaction in Real Seawater, Angew. Chem. Int. Ed. 62 (2023). https://doi.org/10.1002/anie.202309854.

[7] T.X. Nguyen, C.C. Tsai, V.T. Nguyen, Y.J. Huang, Y.H. Su, S.Y. Li, R.K. Xie, Y.J. Lin, J.F. Lee, J.M. Ting, High entropy promoted active site in layered double hydroxide for ultra-stable oxygen evolution reaction electrocatalyst, Chemical Engineering Journal 466 (2023). https://doi.org/10.1016/j.cej.2023.143352.

[8] K. Zhang, R. Zou, Advanced Transition Metal-Based OER Electrocatalysts: Current Status, Opportunities, and Challenges, Small 17 (2021). https://doi.org/10.1002/smll.202100129.

[9] P.M. Bodhankar, P.B. Sarawade, G. Singh, A. Vinu, D.S. Dhawale, Recent advances in highly active nanostructured NiFe LDH catalyst for electrochemical water splitting, J. Mater. Chem. A Mater. 9 (2021) 3180–3208. https://doi.org/10.1039/d0ta10712c.

[10] J. Long, J. Zhang, X. Xu, F. Wang, Crystalline NiFe layered double hydroxide with large pore volume as oxygen evolution electrocatalysts, Mater. Chem. Phys. 254 (2020). https://doi.org/10.1016/j.matchemphys.2020.123496.

[11] J. Jin, J. Xia, X. Qian, T. Wu, H. Ling, A. Hu, M. Li, T. Hang, Exceptional electrocatalytic oxygen evolution efficiency and stability from electrodeposited NiFe alloy on Ni foam, Electrochim. Acta 299 (2019) 567–574. https://doi.org/10.1016/j.electacta.2019.01.026.

[12] A. Sakamaki, M. Yoshida-Hirahara, H. Ogihara, H. Kurokawa, One-Step Synthesis of Highly Active NiFe Electrocatalysts for the Oxygen Evolution Reaction, Langmuir 38 (2022) 5525–5531. https://doi.org/10.1021/acs.langmuir.2c00097.

[13] J. Jia, L. Wei, F. Li, C. Yu, K. Yang, T. Liang, In situ growth of NiFe MOF/NF by controlling solvent mixtures as efficient electrocatalyst in oxygen evolution, Inorg. Chem. Commun. 128 (2021). https://doi.org/10.1016/j.inoche.2021.108605.

[14] G. Luo, H. Feng, R. Zhang, Y. Zheng, R. Tu, Q. Shen, Synthesis of NiFe-layered double hydroxides using triethanolamine-complexed precursors as oxygen evolution reaction catalysts: effects of Fe valence, Dalton Transactions 53 (2024) 1735–1745. https://doi.org/10.1039/d3dt03373b.

[15] C. Sun, Z. Zhang, H. Jang, Z. Li, M.G. Kim, J. Cho, S. Liu, X. Liu, L. Hou, Rational design of nitrate-intercalated NiFe LDH with dual chloride-blocking mechanisms for stable alkaline seawater oxidation, Sci. China Chem. (2026). https://doi.org/10.1007/s11426-025-2983-5.

[16] A. Malek, L. Wu, Y. Li, C. Li, Y. Chen, K. Hazazi, Y. Xue, X. Lu, Transient-Promoter-Stabilized NiFe Oxyhydroxide Enables Durable kW-Scale Water Splitting Under Fluctuating Power, Angew. Chem. Int. Ed. 65 (2026). https://doi.org/10.1002/anie.202520825.

[17] L. Dang, H. Liang, J. Zhuo, B.K. Lamb, H. Sheng, Y. Yang, S. Jin, Direct Synthesis and Anion Exchange of Noncarbonate-Intercalated NiFe-Layered Double Hydroxides and the Influence on Electrocatalysis, Chemistry of Materials 30 (2018) 4321–4330. https://doi.org/10.1021/acs.chemmater.8b01334.

[18] F. Du, J. Yao, H. Luo, Y. Chen, Y. Qin, Y. Du, Y. Wang, W. Hou, M. Shuai, C. Guo, A Cu loaded NiFe layered double hydroxide bifunctional electrocatalyst with a coupled interface structure for both the nitrate reduction reaction and oxygen evolution reaction, Green Chemistry 26 (2023) 895–903. https://doi.org/10.1039/d3gc03823h.

[19] Y. Zhai, X. Ren, Y. Sun, D. Li, B. Wang, S. (Frank) Liu, Synergistic effect of multiple vacancies to induce lattice oxygen redox in NiFe-layered double hydroxide OER catalysts, Appl. Catal. B 323 (2023). https://doi.org/10.1016/j.apcatb.2022.122091.